Article

Current Biology

Creation of an albino squid line by CRISPR-Cas9 and its application for *in vivo* functional imaging of neural activity

Graphical abstract

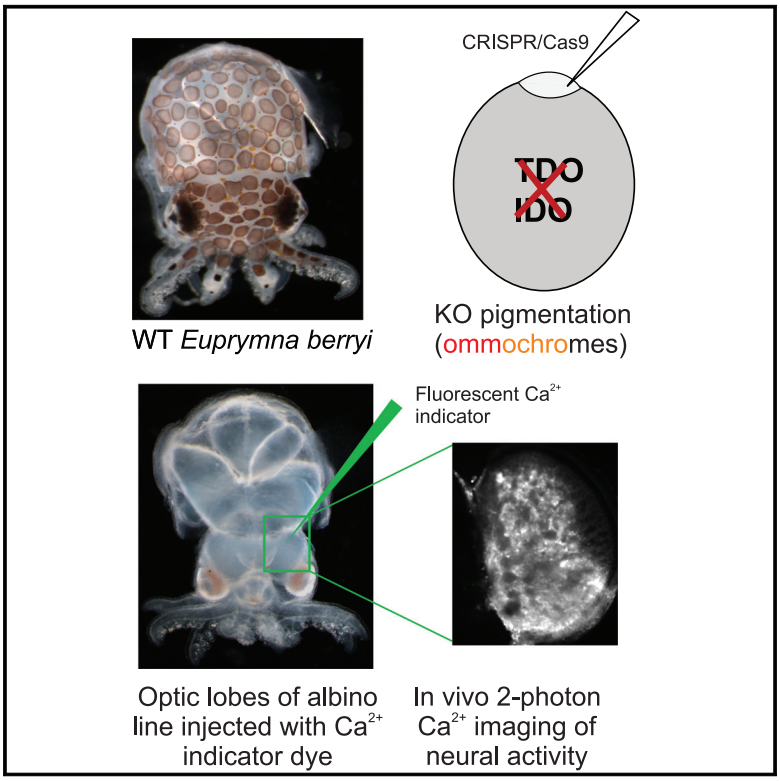

Highlights

- Genetic lines of *Euprymna berryi* can be produced with CRISPR
- The knockout of two pigmentation genes is required to produce albinos
- Neural activity can be imaged non-invasively in the brains of albino lines

Authors

Namrata Ahuja, Ernie Hwaun, Judit R. Pungor, ..., Ivan Soltesz, Caroline B. Albertin, Joshua J.C. Rosenthal

Correspondence

calbertin@mbl.edu (C.B.A.), jrosenthal@mbl.edu (J.J.C.R.)

In brief

Cephalopods are notable for their large nervous systems and complex behaviors. Progress in understanding the underpinnings of these traits has been limited by the lack of a genetically tractable model. Using CRISPR, Ahuja et al. generate albino lines of the squid *Euprymna berryi* and then use them to image neural activity *in vivo*.

Ahuja et al., 2023, Current Biology *33*, 1–10
July 10, 2023
https://doi.org/10.1016/j.cub.2023.05.066

CellPress

Please cite this article in press as: Ahuja et al., Creation of an albino squid line by CRISPR-Cas9 and its application for *in vivo* functional imaging of neural activity, Current Biology (2023), https://doi.org/10.1016/j.cub.2023.05.066

Current Biology

CellPress

Article

Creation of an albino squid line by CRISPR-Cas9 and its application for *in vivo* functional imaging of neural activity

Namrata Ahuja,[1] Ernie Hwaun,[2] Judit R. Pungor,[3] Ruhina Rafiq,[1] Sal Nemes,[1] Taylor Sakmar,[4] Miranda A. Vogt,[4] Bret Grasse,[4] Juan Diaz Quiroz,[1] Tessa G. Montague,[5] Ryan W. Null,[1] Danielle N. Dallis,[4] Daria Gavriouchkina,[6] Ferdinand Marletaz,[7] Lisa Abbo,[4] Daniel S. Rokhsar,[6,8] Cristopher M. Niell,[3] Ivan Soltesz,[2] Caroline B. Albertin,[1,*] and Joshua J.C. Rosenthal[1,9,10,*]

[1]Eugene Bell Center, Marine Biological Laboratory, Woods Hole, MA 02543, USA
[2]Department of Neurosurgery and Stanford Neurosciences Institute, Stanford University, Stanford, CA 94305, USA
[3]Institute of Neuroscience, University of Oregon, Eugene, OR 97403, USA
[4]Marine Resources Center, Marine Biological Laboratory, Woods Hole, MA 02543, USA
[5]Department of Neuroscience, Columbia University, New York, NY 10027, USA
[6]Molecular Genetics Unit, Okinawa Institute of Science and Technology Graduate University, Onna, Okinawa 904-0412, Japan
[7]Centre for Life's Origin & Evolution, Department of Ecology, Evolution & Environment, University College London, WC1E 6BT London, UK
[8]Department of Molecular and Cell Biology, University of California, Berkeley, Berkeley, CA 94720, USA
[9]Twitter: @JoshRosenthal16
[10]Lead contact
*Correspondence: calbertin@mbl.edu (C.B.A.), jrosenthal@mbl.edu (J.J.C.R.)
https://doi.org/10.1016/j.cub.2023.05.066

SUMMARY

Cephalopods are remarkable among invertebrates for their cognitive abilities, adaptive camouflage, novel structures, and propensity for recoding proteins through RNA editing. Due to the lack of genetically tractable cephalopod models, however, the mechanisms underlying these innovations are poorly understood. Genome editing tools such as CRISPR-Cas9 allow targeted mutations in diverse species to better link genes and function. One emerging cephalopod model, *Euprymna berryi*, produces large numbers of embryos that can be easily cultured throughout their life cycle and has a sequenced genome. As proof of principle, we used CRISPR-Cas9 in *E. berryi* to target the gene for tryptophan 2,3 dioxygenase (TDO), an enzyme required for the formation of ommochromes, the pigments present in the eyes and chromatophores of cephalopods. CRISPR-Cas9 ribonucleoproteins targeting *tdo* were injected into early embryos and then cultured to adulthood. Unexpectedly, the injected specimens were pigmented, despite verification of indels at the targeted sites by sequencing in injected animals (G0s). A homozygote knockout line for TDO, bred through multiple generations, was also pigmented. Surprisingly, a gene encoding indoleamine 2,3, dioxygenase (IDO), an enzyme that catalyzes the same reaction as TDO in vertebrates, was also present in *E. berryi*. Double knockouts of both *tdo* and *ido* with CRISPR-Cas9 produced an albino phenotype. We demonstrate the utility of these albinos for *in vivo* imaging of Ca^{2+} signaling in the brain using two-photon microscopy. These data show the feasibility of making gene knockout cephalopod lines that can be used for live imaging of neural activity in these behaviorally sophisticated organisms.

INTRODUCTION

As research organisms, coleoid cephalopods (octopuses, squids, and cuttlefishes) offer unique opportunities to gain a better understanding of the factors that drive behavioral complexity. Coleoids display an independently evolved level of behavioral sophistication that parallels that of many mammals and birds.[1–3] Anatomically, cephalopods' large brain-to-body ratios rival those of vertebrates.[4] Additionally, they display complex cognition[5] in the areas of learning and memory.[6,7] To support these behaviors, coeloid cephalopods evolved a suite of anatomical innovations, including some that are convergent with vertebrates and others that are evolutionary novelties. For example, their camera-type eyes structurally resemble those of vertebrates,[8] helping them to hunt prey and avoid predators.[9] Chromatophore and iridophore organs in their skin produce pigmentary and structural colors that combine to produce exceptional camouflage.[5,10,11] Suckers on their arms serve as multipurpose organs involved in sensory modalities and locomotion.[12,13] Although coleoids possess the largest invertebrate nervous systems, they have more neurons outside of their central brain than within it, most of which are associated with their arms and suckers.[14] These anatomical features, among others, facilitate their advanced behavioral repertoire.

On a molecular level, cephalopods demonstrate multiple diverse innovations as well. Specialized chemotactile receptors,

Please cite this article in press as: Ahuja et al., Creation of an albino squid line by CRISPR-Cas9 and its application for *in vivo* functional imaging of neural activity, Current Biology (2023), https://doi.org/10.1016/j.cub.2023.05.066

some of which likely evolved from acetylcholine receptors, are expressed in the suckers and used to sense poorly soluble compounds.[15] Gene families encoding C2H2 zinc finger proteins and protocadherins have expanded on a massive level, likely to connect their complex nervous systems.[16] In these nervous systems, cephalopods can also recode codons within their mRNA at levels that are orders of magnitude greater than other taxa, providing a novel mechanism for plasticity.[16–23] These coleoid features offer tremendous opportunities to add new perspectives to our understanding of complex cognition. However, the lack of a genetically tractable cephalopod model has been a major obstacle to our ability to study these novelties on a mechanistic level.

Specific characteristics make a given research organism more amenable to genetic manipulation. For example, the species should be culturable throughout its entire life cycle in the lab, provide a reliable source of accessible embryos, have a relatively rapid generation time, and be small to minimize the space required for housing. For organisms that meet these criteria, a high-quality genome assembly and protocols for gene knockout and insertion must be developed to enable functional assays. In a recent study by some of the authors of this work, an effective gene knockout protocol was developed for the squid *Doryteuthis pealeii*, demonstrating the utility of the CRISPR-Cas9 system in these organisms.[24] *D. pealeii*, however, cannot be cultured beyond hatching in the lab, which restricted the knockouts to the injected individuals, which are mosaic, limiting its utility as a model.

In this study, we have turned to *Euprymna berryi*, a bobtail squid from the Indo-Pacific that possesses many important traits for its use as a genetically tractable model system.[25,26] *E. berryi* (1) can be raised in the lab through its entire life cycle, (2) produces frequent clutches of embryos over a 3–4 month span that can be microinjected and then cultured to hatching in an incubator, (3) reaches sexual maturity in about 3 months, (4) has an assembled genome,[27] and (5) is only 3–5 cm in mantle length as an adult.[26,28–30] What is lacking in this emerging model organism is the development of genetic tools and defined genetic strains to facilitate biological discovery. For example, the ability to image neural activity non-invasively is a cornerstone of modern neuroscience and would be an indispensable tool for cephalopod neurobiology. In this study, we produce an albino line of *E. berryi* using CRISPR-Cas9 and demonstrate its utility as a model for neurobiology by recording calcium activity in the central nervous system (CNS) of living specimens using two-photon microscopy.

RESULTS

To create a transparent squid suitable for imaging, we first needed to establish that we could generate knockout lines of *E. berryi* using CRISPR-Cas9. Previously, we developed a protocol for gene knockouts in *D. pealeii*, but these animals were not culturable past hatching.[24] In the *D. pealeii* study, we knocked out the gene encoding tryptophan 2,3, dioxygenase (TDO), an enzyme that catalyzes the first committed step in the biosynthesis of ommochromes, pigments found in the eyes and chromatophores of cephalopods.[31–36] Following a similar logic, our initial goal was to identify the orthologous gene for *tdo* in *E. berryi* and knock it out using the previously established CRISPR-Cas9 protocol. By searching the *E. berryi* genome, we identified an ortholog to *D. pealeii tdo* that comprises 14 exons and 15 introns and spans 153 kilobases (kb) (Figure 1A). As with *D. pealeii*, *E. berryi tdo* is expressed in pigmented tissues (i.e., eyes and chromatophores). During *E. berryi* embryogenesis, pigmentation of the eyes commences at stage 20 and in the chromatophores at stage 26 (using a staging guide for *E. scolopes*[37]). Using embryos at these stages, we performed a whole-mount hybridization chain reaction using probes designed for *E. berryi tdo*. Figure 1B demonstrates strong *tdo* gene expression in the eyes and chromatophores with little to no expression observed elsewhere in the embryo. This pattern is similar to *tdo* expression in *D. pealeii* embryos.[24] These data further supported the idea that *tdo* was an appropriate target to eliminate chromatophore pigmentation.

To make albino *E. berryi*, we designed CRISPR guide RNAs (gRNAs) targeting the *tdo* locus. In total, 3 chemically protected gRNAs were synthesized commercially (Synthego), 2 in exon 9 and 1 in exon 10 (Figure 1A). These gRNAs were microinjected alongside Cas9 protein into cleavage stage (1–8 cells) *E. berryi* embryos (see STAR Methods for a description of embryo preparation). As the first cleavage occurs approximately 8 h following fertilization at 24°C, there was sufficient time to microinject naturally laid embryos (in contrast to *D. pealeii*, which takes ~3.5 h). Each *E. berryi* egg is wrapped in 2 distinct types of jelly that need to be removed before injection, although keeping the chorion intact (Figure 1Ci). This was accomplished using fine forceps, but unlike our methods for *D. pealeii*, we did not need to make partial incisions with micro scissors. As with *D. pealeii*, the blastomere itself needed to be injected, as injections into the yolk were lethal (Figures 1Cii and 1Ciii). After injections, embryos were cultured to hatching, and in some cases beyond, to observe pigmentation.

Surprisingly, embryos injected with *tdo* CRISPR gRNAs and Cas9 appeared mostly pigmented at hatching and very similar to control embryos (Figure 1D). Since no loss of pigmentation was observed, we first suspected that gene knockouts were incomplete; hence, we genotyped five of the experimental individuals by sacrificing them and purifying genomic DNA from the entire animal. Amplicons spanning the CRISPR-directed Cas9 target sites were generated by PCR and skim-sequenced using MiSeq. Disruption of *tdo* in these animals was highly efficient: in exon 9, which contained target sites for 2 CRISPR gRNAs, most individuals had >90% of the *tdo* alleles disrupted (Figure 1E). In exon 10, the site targeted by the other CRISPR gRNA, *tdo* disruptions were less efficient; all animals had <80% of the *tdo* alleles disrupted, with some below 50% disruption, but each animal was confirmed to harbor disruptions in both exons. The pigmentation observed in animals demonstrating a high level of disruption in the *tdo* locus was unexpected, and we reasoned that either the small amount of intact *tdo* was sufficient to generate pigmentation (although this was not the case for similar experiments in *D. pealeii*) or sufficient quantities of N-formylkynurenine for ommochrome biosynthesis was being produced by another copy of *tdo*, a different *tdo* isoform, or a different enzyme.

To test whether the small fraction of intact *tdo* was sufficient for pigmentation in the G0 hatchlings, we bred a homozygous

Please cite this article in press as: Ahuja et al., Creation of an albino squid line by CRISPR-Cas9 and its application for *in vivo* functional imaging of neural activity, Current Biology (2023), https://doi.org/10.1016/j.cub.2023.05.066

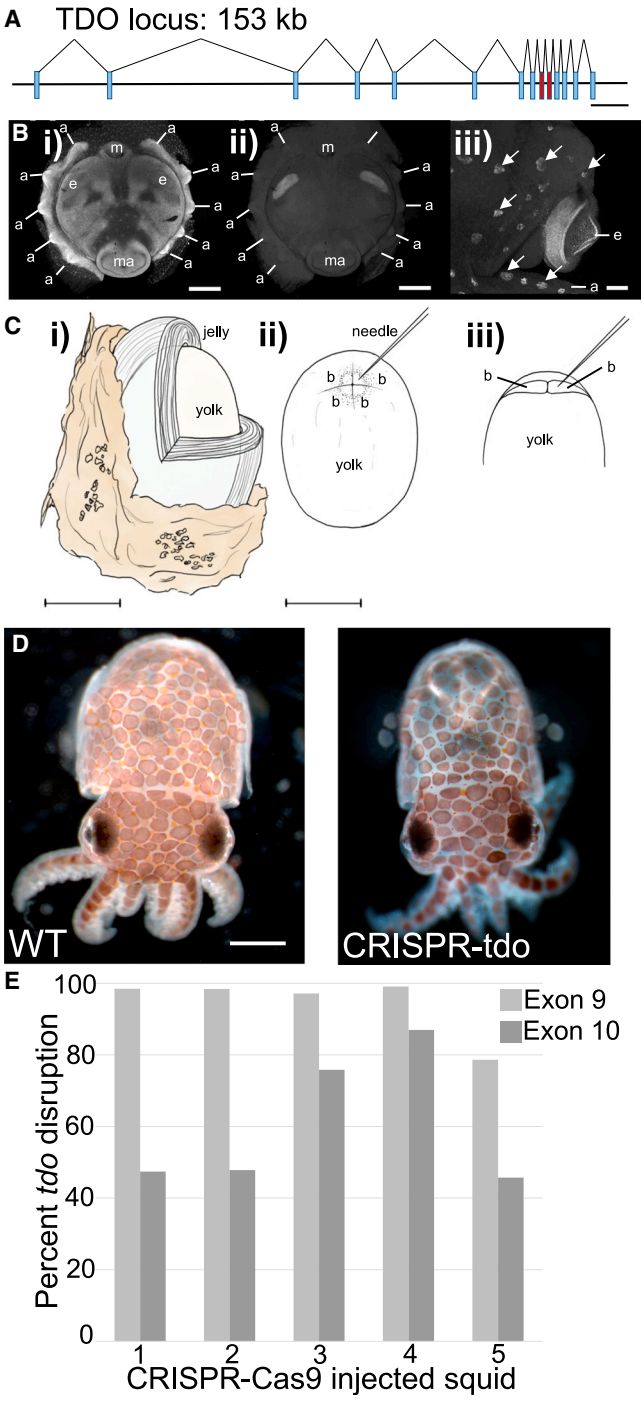

Figure 1. CRISPR-Cas9-mediated mutagenesis of *TDO* in *E. berryi*

(A) Schematic of the *E. berryi TDO* locus showing 15 exons and 14 introns. gRNAs target exons 9 and 10 (red); scale bar, 10 kb. See also Figure S1.

(B) Hybridization chain reaction *in situ* hybridizations for *tdo* expression in *E. berryi* embryos. (i) DAPI staining and (ii) *tdo* expression (scale bars, 500 μM) in a stage 20 *E. berryi* embryo illustrate *tdo* expression in the developing eye primordium. (iii) A close-up of a stage 27 embryo shows *tdo* eye and chromatophore expression (scale bars, 100 μM). M, mouth; a, arm primordia; ma, mantle; e, eye; arrows point to chromatophores.

(C) Cartoon images of cleavage stage *E. berryi* embryos. (i) Illustration of an embryo covered in two types of jelly: the tunic (tan) and jelly layers (gray) surrounding the yolky embryo, contained in a chorion. (ii) Animal pole view of an embryo at the 4-cell stage with a quartz injection needle piercing one of the cells. (iii) Embryo at the 2-cell stage with needle injecting through chorion and into 1 of the cells. Individual cells labeled as "b." Scale bar, ~1 mm.

(D) Images of *E. berryi* at hatching stage. Left image shows a wild-type (WT) phenotype. Right image shows a squid injected with Cas9 and gRNAs targeting *tdo* exons 9 and 10. Scale bar, 230 μm.

(E) Percent *tdo* disruption in exons 9 and 10 (where guides are located) in 5 CRISPR-Cas9 injected *E. berryi*. Percent disruption was calculated from PCR amplicons spanning the two CRISPR gRNA cut sites using genomic DNA extracted from whole hatchlings.

knockout line. To accomplish this, we raised G0 animals to sexual maturity and in-crossed 7 pairs. F1 animals from each cross were then genotyped. Four of the crosses only produced wild-type (WT) animals, but 3 crosses produced heterozygotes containing a wide variety of indels among the genotyped individuals. The numbers of heterozygous and WT animals for the three crosses were as follows: 4 heterozygotes and 3 WT, 6 heterozygotes and 3 WT, and 3 heterozygotes and 13 WT, for a total of 13 heterozygotes and 19 WT. One of the F1 progeny that contained a 7 base pair (bp) deletion in exon 9 was used to produce a homozygous knockout line. To avoid inbreeding depression from sibling crosses and possible accumulations of off-target CRISPR mutations, we first outcrossed the 7 bp deletion F1 heterozygote with a WT from a different parental line. F2s from this pairing were genotyped and heterozygotes were identified with the same 7 bp deletion and in Mendelian ratios. F2 heterozygotes from separate lineages were crossed to create an F3 line, which we expected to produce some homozygous knockout *tdo* animals (Figure 2A). To confirm the genotypes of F3 animals, the 7 bp deletion was verified via sequencing. Although we recovered genotypes that aligned with the expected Mendelian ratios (Figure 2B), the homozygote *tdo* knockout squid were still visually pigmented (Figure 2C).

Although $tdo^{-/-}$ animals were fully pigmented at hatching, pigmentation was slightly delayed. WT animals begin to develop pigment in their eyes during embryogenesis around stage 20 (specific stages are in reference to the *E. scolopes* embryo guide[37]; 8/9 dpf at 24°C) and in their chromatophores at stage 26 (13/14 dpf at 24°C). Normally, the chromatophores and eyes quickly darken to brown and black by stage 28 (18 dpf) and 26 (15–16 dpf), respectively. However, in some F3 animals at these two stages, coloration was less well developed (Figure 2D, arrow). Eyes took longer to develop color, staying a light orange and then a red before eventually turning black at stage 28; chromatophores stayed red past stage 26 until stage 28, when they transitioned to brown. This was close to hatching (stage 30, 24 dpf). The animals displaying the delayed pigmentation phenotype were genotyped and found to be $tdo^{-/-}$. This led us to believe that there was either another copy of *tdo* or another enzyme capable of producing N-formylkynurenine (the first committed step in the production of ommochrome pigments from tryptophan) in the genome. Searches of the genome, however, did not uncover additional copies of *tdo*, or other *tdo* isoforms. In addition, because ommochromes are highly conserved across cephalopods, we considered it unlikely that another pigment type was responsible for coloration.

Indoleamine 2,3 dioxygenase (IDO) is structurally distinct from TDO but is known to catalyze the same reaction in many vertebrates and some mollusks.[38–43] Although *ido* homologs were

Please cite this article in press as: Ahuja et al., Creation of an albino squid line by CRISPR-Cas9 and its application for *in vivo* functional imaging of neural activity, Current Biology (2023), https://doi.org/10.1016/j.cub.2023.05.066

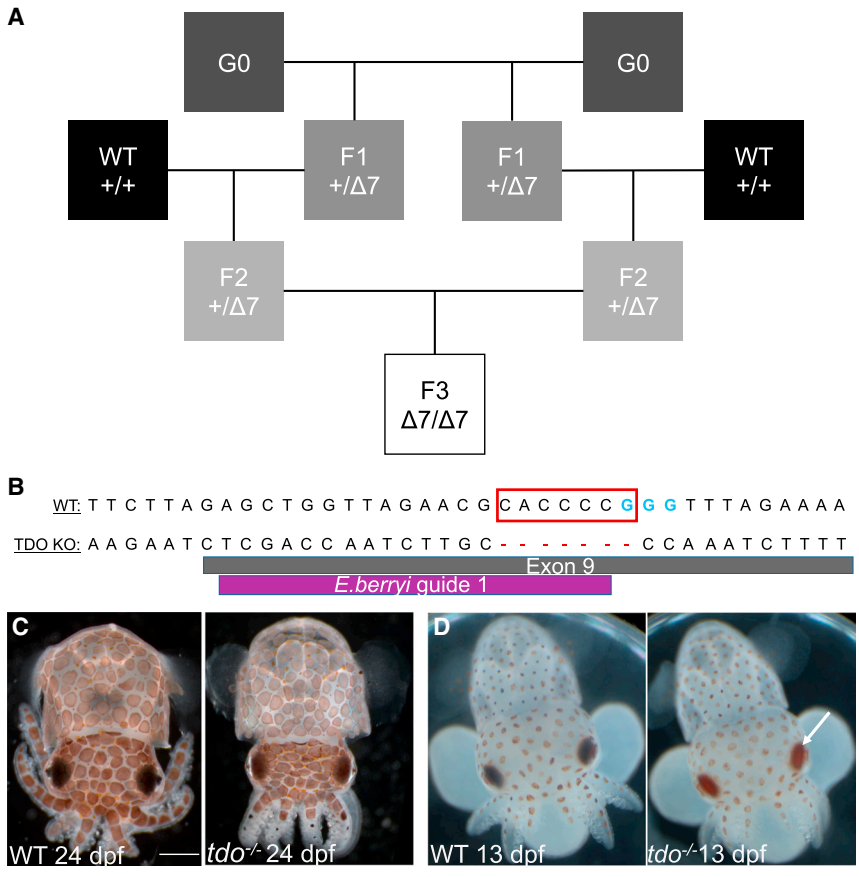

Figure 2. Generation of a *TDO* knockout line in *E. berryi*

(A) Illustration of crosses used to create a homozygote line for tdo$^{-/-}$ through the F3 generation.

(B) Alignment of a tdo$^{+/+}$ (WT) sequence (top) with a tdo$^{-/-}$ knockout sequence (bottom) in exon 9. Purple bar indicates location of the gRNA target. Nucleotides in red box are deleted in the TDO knockouts. The CRISPR protospacer adjacent motif site, which is required for Cas9 to cut, is highlighted in blue.

(C) Images of *E. berryi* squid at hatching, left showing a WT hatchling and right showing a tdo$^{-/-}$ knockout hatchling at 24 dpf. Scale bar, 230 μm.

(D) *E. berryi* WT and tdo$^{-/-}$ knockout embryos at 13 dpf. Scale bar, 230 μm.

not seen in the *D. pealeii* genome, we did identify a putative homolog in the *E. scolopes* and *E. berryi* genomes. Trees containing both TDO and IDO sequences confirm a bona fide IDO encoded in *Euprymna* genomes (Figure S1). *E. berryi ido* is composed of 12 exons and 11 introns, spanning a total of 108 kb (Figure 3A). To confirm that IDO is indeed expressed in *E. berryi*, we confirmed the presence of transcripts using RT-PCR on RNA extracted from whole stage 24 embryos (data not shown). To examine the spatial expression of *ido*, we attempted to localize it using the same HCR methods used for *tdo* but were unsuccessful. We hypothesized that this might be due to low expression levels for IDO. Indeed, qPCR experiments using cDNA from stage 24 embryos indicated that *ido* expression is close to 40 times lower than that of *tdo* (Figure 3B).

To determine whether *E. berryi* IDO contributes to ommochrome biosynthesis, we first attempted to knockout the *ido* gene using the same approach that was used to knockout *tdo* (in this case 2 gRNAs were injected (STAR Methods). For *ido*, both CRISPR gRNAs targeted exon 3 (Figure 3A). These were injected into early-stage embryos along with Cas9 enzyme. As with the *tdo* injected animals before, hatchling G0 animals exhibited no loss of pigmentation and looked similar to the WT animals (Figure 3C). Next, we hypothesized that the activity of each enzyme could compensate for the other. To test this idea, we attempted to knockout both *tdo* and *ido* simultaneously. First, we tried injecting homozygote tdo$^{-/-}$ embryos with *ido* gRNAs, but this, for unknown reasons, resulted in deformed embryos that rarely survived to hatching. Next, we co-injected *tdo* and *ido* CRISPR guides (gRNA3 for *tdo*, which was the most efficient, and both *ido* gRNAs). During the development of the double knockout G0 embryos, many specimens exhibited a mosaic pigmentation phenotype, and some were complete albinos (Figure 4A). The mosaicism resulted in combinations of red instead of black eyes, red chromatophores, or a complete loss of chromatophore pigmentation. Fully transparent squid, unfortunately, did not survive longer than ~3 weeks post-hatching. To make a genetic strain of albino squid, we crossed 2 adult G0 animals injected with guides to both *tdo* and *ido* that demonstrated mosaic pigmentation. The F1s from this cross resulted in red-eyed, WT, and full albino phenotypes (Figure 4B). We genotyped animals from each of these phenotypes to correlate phenotype with genotype (Figure 4C). Albino squid were confirmed to be homozygous knockouts for both genes. The red-eyed phenotype is produced in full *tdo* knockouts with either a heterozygous or WT *ido*. The genotypes for animals with WT pigmentation were tdo$^{+/+}$ ido$^{+/+}$, tdo$^{+/+}$ ido$^{+/-}$, tdo$^{+/-}$ ido$^{+/-}$, and tdo$^{+/+}$ ido$^{-/-}$. Albino animals did not survive well after hatching: most died within a week, presumably because they fed poorly due to difficulties catching prey. A few animals that were hand-fed multiple times per day survived about a month.

The albino *E. berryi* are nearly transparent (Figure 4B). This transparency makes them an ideal model to study neural activity using fluorescent markers. Unfortunately, since albinos did not survive to adulthood, we carried out further experiments with hatchlings within 1 week post-hatching. However, red-eyed and WT animals are culturable through their life cycles. Thus, production of additional albinos requires crosses of some combination of the two red-eyed genotypes and WT animals of the tdo$^{+/-}$ ido$^{+/-}$ genotype. These albino animals were then used for neuroimaging.

Imaging of neural activity in the brains of albino *E. berryi in vivo*

The transparency of the albino *E. berryi* presents an opportunity to study neural activity *in vivo* using fluorescent indicators of

Please cite this article in press as: Ahuja et al., Creation of an albino squid line by CRISPR-Cas9 and its application for *in vivo* functional imaging of neural activity, Current Biology (2023), https://doi.org/10.1016/j.cub.2023.05.066

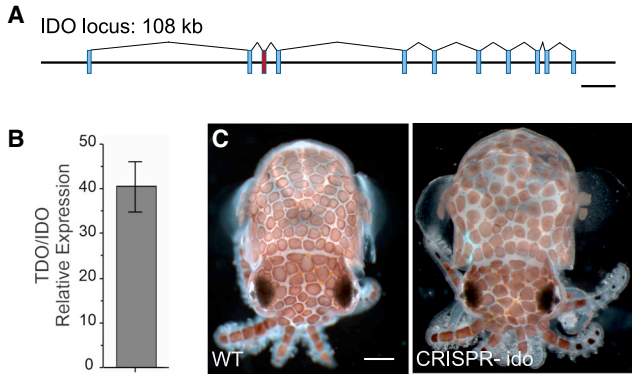

Figure 3. CRISPR-Cas9-mediated knockout of *IDO* in *E. berryi*

(A) A schematic of the *ido* locus in *E. berryi* with 11 exons, 12 introns, and gRNAs located in exon 3 (red). Scale bar, 10 kb. See also Figure S1.

(B) Relative expression of *tdo* and *ido* in wild-type stage 24 embryos determined from qPCR on whole embryo cDNA. Relative expression determined from average Qp cycles for each message (5 biological replicates).

(C) Images of a WT *E. berryi* hatchling (left) versus one injected with a CRISPR gRNA targeting *ido* and Cas9 (right). Scale bar, 270 μm.

neuronal activity. To demonstrate this utility for studying neural dynamics, we used preparation for *in vivo* two-photon calcium imaging of optic lobes.[44] One advantage of choosing the optic lobes to validate our imaging approach is that neural activity can be triggered by noninvasive visual stimuli. We first injected the calcium indicator Cal-520 into the optic lobes of anesthetized albino squid hatchlings using a beveled quartz micropipette (Figures 5A and 5B). To constrain movement after recovery from anesthesia, we embedded the whole squid in 4% agarose in artificial seawater (ASW). Embedded animals were then placed in a recording chamber filled with ASW. Visual stimuli were projected onto a white screen located on one side of the recording chamber, ipsilateral to the optic lobe that was imaged. The objective of the two-photon microscope was immersed in ASW to image calcium responses in the optic lobes. The calcium dye was successfully loaded into the cells in the optic lobes, as evidenced by the recorded baseline fluorescence (Figure 5C).

Visual stimuli reliably triggered a calcium response in part of the optic lobe (Figures 5D–5F), demonstrating the feasibility of studying neural activity in intact cephalopods for the first time. Visually evoked calcium responses in the optic lobe were not spatially homogeneous, as parts of the optic lobe remained silent following the presentation of visual stimuli despite the successful loading of calcium indicator dye. The time delay to reach maximum fluorescence after the stimulus onset (Figures 5D and 5F), however, excludes the possibility that the signals were due to background illumination produced by the stimulus alone. In fact, the average calcium signal in the active region persisted for more than 1 s after the stimulus offset (Figure 5F), consistent with calcium and indicator dynamics. In total, we loaded the calcium dye into the optic lobes of four different albino squid and observed a variable proportion of optic lobes being active when visual stimuli were presented (Figure 5G), illustrating the repeatability of the approach as well as the inter-animal variability in the robustness of the imaging signal.

Finally, to illustrate the advantage of using albino squid for *in vivo* imaging, we performed the same two-photon calcium imaging experiment on WT animals (Figure 6). Not surprisingly, the pigmented chromatophores on the WT specimens obstructed the two-photon laser illumination and prevented imaging sections of the optic lobe underneath, whereas clear unobstructed imaging of the entire optic lobe was possible in the albinos.

DISCUSSION

This study presents several key advances for studying cephalopod biology, particularly in the areas of development and neurobiology. First, we introduce *E. berryi* as a model for molecular genetics. Previous work has demonstrated the potential utility of this species[26]: it is small, reaches sexual maturity relatively rapidly (3–4 months, depending on the culture temperature), and is robust in culture. *E. berryi* displays similar characteristics to *Euprymna scolopes*, a morphologically comparable congener that has been an important and well-studied model for bacterial-animal symbioses.[45] Both *Euprymna* species are of a similar size, possess light organs that harbor luminescent bacteria, are docile in captivity, and are culturable throughout their life cycle. We chose to focus on *E. berryi* for this work because, in our hands, they have a much higher survival rate immediately after hatching, a critical period in cephalopod husbandry. Using *E. berryi* and CRISPR-Cas9, we produced defined gene knockout lines, a first for cephalopod biology, and we continue to culture these lines over multiple generations. These steps are prerequisites to the application of modern biological tools to the study of cephalopods.

Surprisingly, our attempts to knockout pigmentation in *E. berryi* suggested the presence of a second gene in the pigmentation pathway that is absent in another distantly related squid, *D. pealeii*. It is well accepted that the pigments in cephalopod chromatophores and retinas are ommochromes.[34–36] The first committed step in their biosynthesis involves the conversion of tryptophan to formylkynurenine, a reaction catalyzed by TDO. Indeed, the knockout of *tdo* in *D. pealeii* completely inhibited pigmentation but had little to no effect on *E. berryi*. We identified a gene encoding IDO, an enzyme that catalyzes the same reaction, in this species. BLAST searches failed to identify *ido* orthologs in the genome of *D. pealeii*[16,23] but did uncover one in *E. scolopes*[46] and *E. berryi*. Using *in situ* hybridization, we were unable to detect *ido* gene expression in the chromatophores and eyes of stage 24 *E. berryi* embryos, a developmental stage that marks the onset of pigmentation. However, qPCR indicated *ido* expression is ~40 times lower than that of *tdo* at this stage (Figure 3B). This suggests that while TDO is the main catalyst of formylkynurenine production for ommochrome biosynthesis in squids, IDO can compensate in the absence of TDO in lineages with both genes.

Notably, IDO is not uniformly detected across mollusks but has been identified in pond snails and abalone, among others.[41,47] IDO is largely absent in arthropod genomes, and although its function in invertebrates is not well understood, it has been studied more thoroughly in vertebrates. In vertebrates, it plays a critical role in tryptophan metabolism and its dysregulation has been linked to diverse pathologies, such as inflammatory bowel disease, CNS disorders, and cancer.[48–52] A better understanding of IDO expression in squids may

Please cite this article in press as: Ahuja et al., Creation of an albino squid line by CRISPR-Cas9 and its application for *in vivo* functional imaging of neural activity, Current Biology (2023), https://doi.org/10.1016/j.cub.2023.05.066

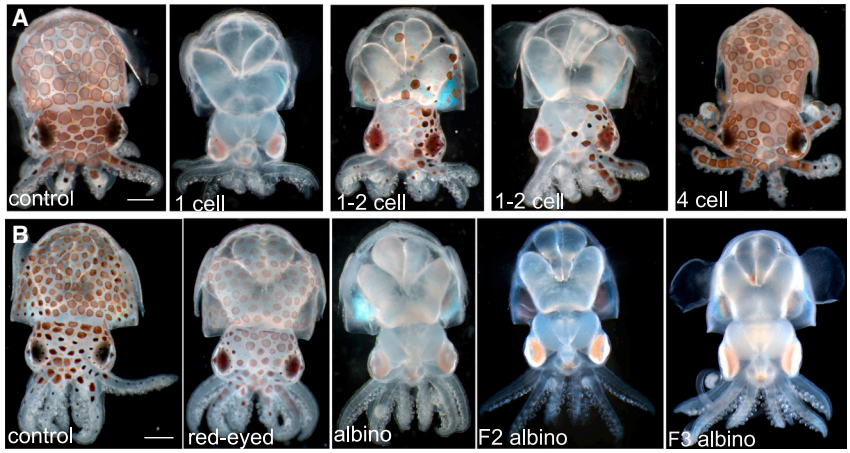

Figure 4. Generation of albino *E. berryi* by knocking out both TDO and IDO

(A) Mosaic phenotypes of G0 hatchlings injected with gRNAs targeting both *ido* and *tdo* at 1 cell, 1–2 cells, and 4 cell stages, versus a wild-type squid. Scale bar, 0.40 μM.

(B) *E. berryi* F1 phenotypes produced by crossing 2 mosaic G0s (A). "Red-eyed" phenotypes show subtle pigmentation loss in the eyes. Albino phenotypes lack pigmentation in both the eyes and chromatophores. For comparison, a WT control is shown in the left-most panel. Scale bar, 0.40 μM.

(C) Table showing the correlation between phenotypes and genotypes in an F2 cross of two red-eyed specimens. n, the number of each phenotype out of 35 specimens.

C

Phenotype	TDO genotype	IDO Genotype	n
Albino	$tdo^{-/-}$	$ido^{-/-}$	3
Red-eyed	$tdo^{-/-}$	$ido^{+/+}$	7
Red-eyed	$tdo^{-/-}$	$ido^{+/-}$	5
WT	$tdo^{+/-}$	$ido^{+/-}$	8
WT	$tdo^{+/-}$	$ido^{+/+}$	1
WT	$tdo^{+/+}$	$ido^{-/-}$	1
WT	$tdo^{+/+}$	$ido^{+/-}$	8
WT	$tdo^{+/+}$	$ido^{+/+}$	2

provide clues about its physiological role. This study demonstrated that the absence of both TDO and IDO is lethal as albino animals died post-hatching. They appeared to be unable to capture prey but could be kept alive up to ~4 weeks after hatching if they were manually fed several times a day. It should be noted that *tdo* and *ido* single and double knockouts are tolerated in mice.[53] In *E. berryi*, the lack of eye pigmentation may impair vision, leading to difficulties in hunting their prey, but other deficits related to tryptophan metabolism may cause or contribute to the lethal phenotype. However, these lines are easily maintained with heterozygote animals, which can be crossed to produce albinos that are suitable for study for the first few weeks post-hatching.

The lines produced in this study are not only valuable for exploring squid coloration but will also be a useful tool for neurobiological studies. Albino *E. berryi* is nearly transparent, providing clear optical access for visualizing the CNS in intact animals. We demonstrate the utility of this transparency with two-photon imaging of neural response to visual stimuli using an injected fluorescent calcium indicator. The embedding of the animals recovering from anesthesia in agarose resulted in sufficient mechanical stability to enable functional calcium imaging in the optic lobe *in vivo*. Importantly, visual stimuli evoked reproducible increases in calcium indicator fluorescence, with the responses time-locked to the stimulus onset and maintained throughout stimulus duration in most cases. Although it was possible to achieve clear imaging of the entire optic lobe in the albino squid, pigments in the WTs typically obstructed optical access.

This minimally invasive approach will enable functional studies of the cephalopod nervous system. To this end, an important next step will be to establish protocols to drive the expression of state-of-the-art calcium and voltage indicators of neuronal activity, either via establishing transgenic lines of genomically encoded reporters or via a transient mechanism of driving reporter expression (e.g., mRNA or plasmid injection, electroporation, or via a viral vector). Moreover, with recent single-cell RNA sequencing experiments revealing diverse functional cell types in the cephalopod brains[27,54,55] and new genetic tools leveraging RNA editing to achieve cell-type-specific gene expression,[56] future experiments would soon be able to interrogate functional properties of microcircuits using our albino animals.

STAR★METHODS

Detailed methods are provided in the online version of this paper and include the following:

- KEY RESOURCES TABLE
- RESOURCE AVAILABILITY
  - Lead contact
  - Materials availability
  - Data and code availability
- EXPERIMENTAL MODEL AND SUBJECT DETAILS
- METHOD DETAILS
  - Embryo collection and preparation
  - Embryo Injection
  - CRISPR-Cas9 injection mixes

Please cite this article in press as: Ahuja et al., Creation of an albino squid line by CRISPR-Cas9 and its application for *in vivo* functional imaging of neural activity, Current Biology (2023), https://doi.org/10.1016/j.cub.2023.05.066

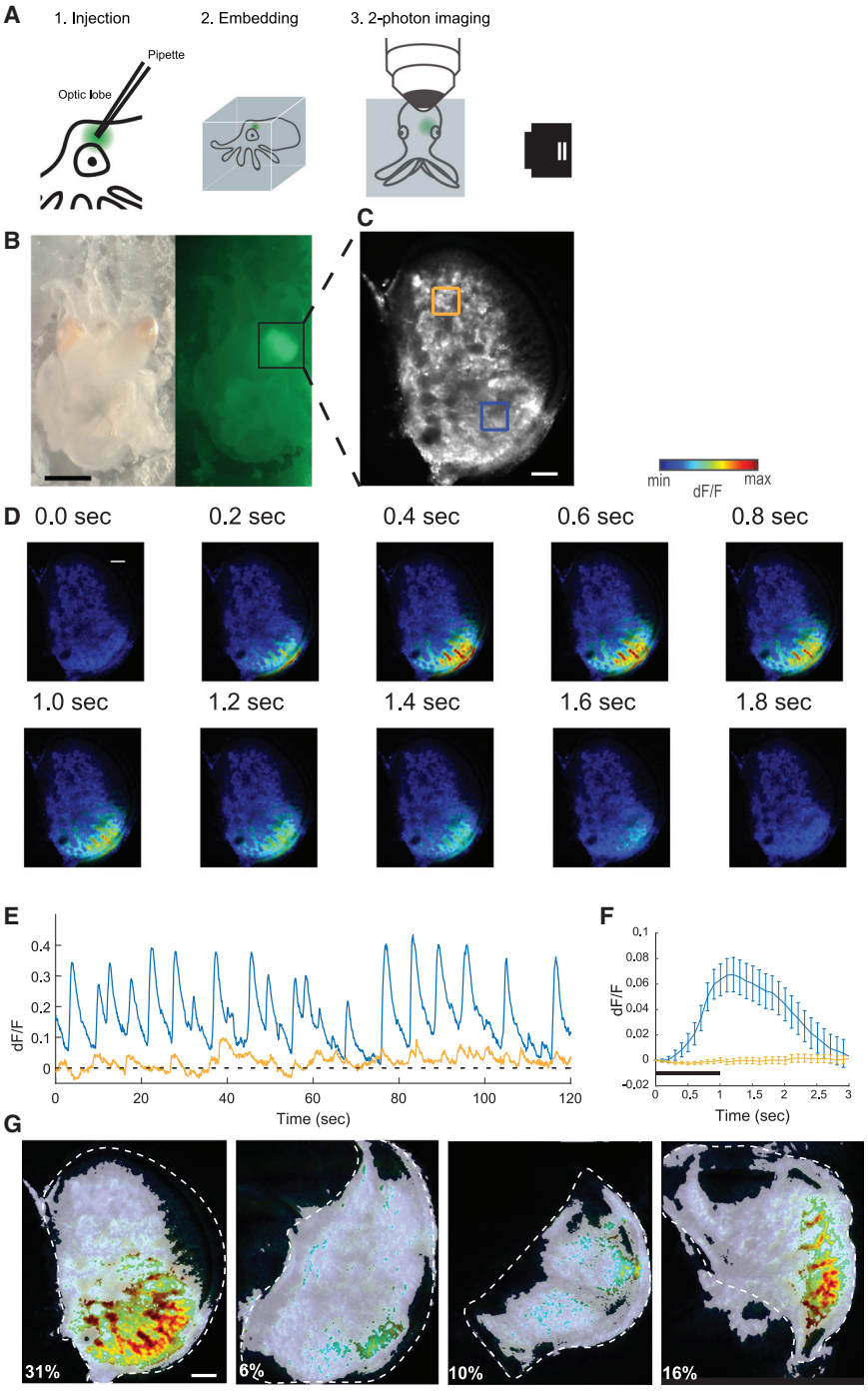

Figure 5. Albino squid enable two-photon imaging of optic lobes *in vivo*

(A) A schematic showing two-photon imaging preparation of living squid. Anesthetized squid were first glued on a cover glass for calcium dye (Cal-520 AM) injection into the optic lobes. Next, the squid were embedded in 4% agarose to constrain movement. Artificial seawater was added to the chamber to allow the squid to recover from anesthesia. Finally, the constrained squid were placed under a two-photon microscope for live imaging, whereas visual stimuli were displayed on a white screen on one side of the recording chamber.

(B) Photograph of an albino *E. berryi* injected with the calcium indicator Cal-520, under bright-field illumination (left) and epifluorescence (right), showing loading of the indicator in the right optic lobe (black square box). Scale bars, 1 mm.

(C) A mean image of the loading of injected calcium dye in the optic lobe. Two boxed regions of interest (ROIs) are analyzed in the following panels.

(D) Average activation across the optic lobe over the course of a square-wave grating visual stimulus. The color map represents change in fluorescence intensity, with hotter colors corresponding to a greater increase. Stimulus onset is at 0 s, offset at 1 s, showing the rise and decay of calcium response over time. Scale bar, 100 μm.

(E) dF/F of each of the boxed ROIs in (C) within an example section of a recording. Blue and orange traces represent the average activity within the blue and orange boxes, respectively. Black bars denote timing of presentation of square-wave grating stimuli, interspersed with gray screen inter-stimulus intervals. The area within the blue ROI shows stimulus locked activation, whereas the area in orange does not.

(F) Average dF/F of ROIs to stimulus presentations. Black bar denotes stimulus presentation duration. The blue trace shows the response of a region triggered by visual stimuli, whereas the orange trace shows a lack of response in an area of the optic lobe that was loaded with calcium indicator but was not sensitive to the stimuli presented. Error bars indicate SEM.

(G) Results from two-photon imaging sessions of optic lobes from four different albino squid. The white shaded area highlights the regions of the optic lobes loaded with calcium dye, while the color scale reflects average changes in dF/F when visual stimuli are presented. Colored regions without shading indicate the areas with significant increase in dF/F, and the percentages out of total area loaded with calcium dye are shown on the bottom left. White dashed lines outline optic lobes. Scale bar, 100 μm.

- Identifying TDO and IDO in *E. berryi*
- Hybridization Chain Reaction
- Quantification of TDO and IDO expression by qPCR
- Genotyping
- *E. berryi* embryo culture
- Calcium Dye Injection
- Visual stimuli

● QUANTIFICATION AND STATISTICAL ANALYSIS

SUPPLEMENTAL INFORMATION

Supplemental information can be found online at https://doi.org/10.1016/j.cub.2023.05.066.

ACKNOWLEDGMENTS

This research was supported by NSF EDGE 2220587 (C.B.A. and J.J.C.R.), NSF EDGE 1827509 (J.J.C.R. and C.B.A.), NSF-BSF 2110074 (J.J.C.R.),

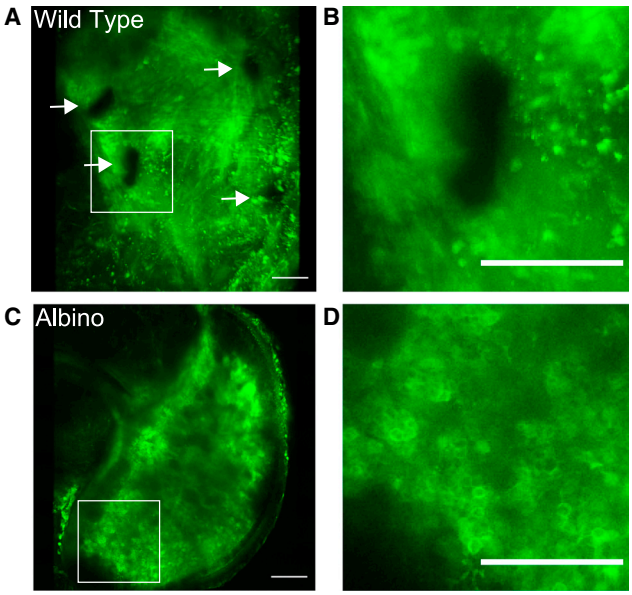

Figure 6. Albino squid provide clear optical access to optic lobes

(A) The optic lobe of wild-type *E. berryi* was loaded with the calcium indicator Cal-520. The image was produced by maximum intensity projection of a 300 mm z stack. White arrows point to pigments on the skin surface that obstruct the image. Note the chromatophores were highly constricted during the experiment.

(B) Magnified view of the white square in (A) is shown.

(C and D) Same as in (A) and (B), but for albino *E. berryi*. Note a lack of black spots over the optic lobe that would have blocked the image and the presence of clear circular shapes that reflect successful imaging of the cells loaded with Cal-520. Scale bars, 100 μm.

NSF 1723141 (J.J.C.R.), NIH R35GM147273-01 (C.B.A.), NIH R01NS118466-01 (C.M.N.), ONR N00014-21-1-2426 (C.M.N.), ONR MURI grant N0014-19-1-2373 (I.S.), Wu Tsai Neurosciences Institute Interdisciplinary Scholarship Award (E.H.), and BSF 2013094 (J.J.C.R.). C.B.A. is supported by the Hibbitt Early Career Fellowship at the Marine Biological Laboratory. We thank Jeffrey Jolly, Ryuta Nakajima, and Seishi Nakano from Yokayoka Diving Service for invaluable help in procuring the *E. berryi* founder populations for this study. We thank the Cephalopod Program at the MBL for their support.

AUTHOR CONTRIBUTIONS

N.A. performed all CRISPR experiments. E.H. and J.R.P. performed live imaging experiments. N.A., R.R., L.A., and S.N. helped with genotyping and the care of injected embryos. J.D.Q. performed bioinformatics analysis to quantify CRISPR disruptions. T.S., M.A.V., B.G., and D.N.D. performed all the husbandry for *E. berryi* specimens, both maintaining CRISPR animals and producing embryos. T.G.M. helped establish microinjection techniques. D.G., F.M., and D.S.R. provided DNA sequences for the *E. berryi* TDO and IDO gene models. R.W.N. performed and imaged the *in situ* hybridizations. N.A., J.J.C.R., and C.B.A. designed and implemented all CRISPR experiments. E.H., J.R.P., C.M.N., and I.S. designed and implemented all live imaging experiments. N.A., C.B.A., J.J.C.R., E.H., J.R.P., C.M.N., and I.S. wrote the manuscript with editorial contributions from T.G.M. and D.S.R.

DECLARATION OF INTERESTS

The authors declare no competing interests.

INCLUSION AND DIVERSITY

We support inclusive, diverse, and equitable conduct of research. One or more of the authors of this paper self-identifies as an underrepresented ethnic minority in their field of research or within their geographical location. One or more of the authors of this paper self-identifies as a member of the LGBTQIA+ community. One or more of the authors of this paper received support from a program designed to increase minority representation in their field of research.

Received: February 23, 2023
Revised: May 17, 2023
Accepted: May 26, 2023
Published: June 20, 2023

REFERENCES

1. Schnell, A.K., Amodio, P., Boeckle, M., and Clayton, N.S. (2021). How intelligent is a cephalopod? Lessons from comparative cognition. Biol. Rev. Camb. Philos. Soc. *96*, 162–178. https://doi.org/10.1111/brv.12651.
2. Edelman, D.B., and Seth, A.K. (2009). Animal consciousness: a synthetic approach. Trends Neurosci. *32*, 476–484. https://doi.org/10.1016/j.tins.2009.05.008.
3. Amodio, P., Boeckle, M., Schnell, A.K., Ostojíc, L., Fiorito, G., and Clayton, N.S. (2019). Grow smart and die young: why did cephalopods evolve intelligence? Trends Ecol. Evol. *34*, 45–56. https://doi.org/10.1016/j.tree.2018.10.010.
4. Packard, A. (1972). Cephalopods and fish: the limits of convergence. Biol. Rev. *47*, 241–307. https://doi.org/10.1111/j.1469-185X.1972.tb00975.x.
5. Hanlon, R., and Messenger, J.B. (2018). Cephalopod Behavior (Cambridge University Press).
6. Sanders, G.D. (1975). The cephalopods. In Invertebrate Learning (Springer), pp. 1–101. https://doi.org/10.1007/978-1-4684-3012-7_1.
7. Wells, M.J. (1978). Octopus (Springer Netherlands). https://doi.org/10.1007/978-94-017-2468-5.
8. Muntz, W.R.A. (1999). Visual systems, behaviour, and environment in cephalopods. In Adaptive Mechanisms in the Ecology of Vision, S.N. Archer, M.B.A. Djamgoz, E.R. Loew, J.C. Partridge, and S. Vallerga, eds. (Springer Netherlands), pp. 467–483. https://doi.org/10.1007/978-94-017-0619-3_15.
9. Yoshida, M.A., and Ogura, A. (2011). Genetic mechanisms involved in the evolution of the cephalopod camera eye revealed by transcriptomic and developmental studies. BMC Evol. Biol. *11*, 180. https://doi.org/10.1186/1471-2148-11-180.
10. Messenger, J.B. (2001). Cephalopod chromatophores: neurobiology and natural history. Biol. Rev. Camb. Philos. Soc. *76*, 473–528. https://doi.org/10.1017/S1464793101005772.
11. Packard, A. (1995). Organization of cephalopod chromatophore systems: a neuromuscular image-generator. In Cephalopod Neurobiology: Neuroscience Studies in Squid, Octopus and Cuttlefish (Oxford University Press), pp. 331–368. https://doi.org/10.1093/acprof:oso/9780198547907.003.0226.
12. Packard, A. (1988). The skin of cephalopods (coleoids): general and special adaptations. In Form and Function (Elsevier), pp. 37–67. https://doi.org/10.1016/B978-0-12-751411-6.50010-2.
13. Wells, M.J., Freeman, N.H., and Ashburner, M. (1965). Some experiments on the chemotactile sense of octopuses. J. Exp. Biol. *43*, 553–563. https://doi.org/10.1242/jeb.43.3.553.
14. Young, J.Z. (1963). The number and sizes of nerve cells in *octopus*. Proc. Zool. Soc. Lond. *140*, 229–254. https://doi.org/10.1111/j.1469-7998.1963.tb01862.x.
15. van Giesen, L., Kilian, P.B., Allard, C.A.H., and Bellono, N.W. (2020). Molecular basis of chemotactile sensation in octopus. Cell *183*, 594–604.e14. https://doi.org/10.1016/j.cell.2020.09.008.
16. Albertin, C.B., Simakov, O., Mitros, T., Wang, Z.Y., Pungor, J.R., Edsinger-Gonzales, E., Brenner, S., Ragsdale, C.W., and Rokhsar, D.S. (2015). The octopus genome and the evolution of cephalopod neural and morphological novelties. Nature *524*, 220–224. https://doi.org/10.1038/nature14668.

17. Alon, S., Garrett, S.C., Levanon, E.Y., Olson, S., Graveley, B.R., Rosenthal, J.J.C., and Eisenberg, E. (2015). The majority of transcripts in the squid nervous system are extensively recoded by A-to-I RNA editing. eLife *4*, e05198. https://doi.org/10.7554/eLife.05198.

18. Colina, C., Palavicini, J.P., Srikumar, D., Holmgren, M., and Rosenthal, J.J.C. (2010). Regulation of Na+/K+ ATPase transport velocity by RNA editing. PLoS Biol. *8*, e1000540. https://doi.org/10.1371/journal.pbio.1000540.

19. Garrett, S., and Rosenthal, J.J.C. (2012). RNA editing underlies temperature adaptation in K^+ channels from polar octopuses. Science *35*, 848–851. https://doi.org/10.1126/science.1212795.

20. Liscovitch-Brauer, N., Alon, S., Porath, H.T., Elstein, B., Unger, R., Ziv, T., Admon, A., Levanon, E.Y., Rosenthal, J.J.C., and Eisenberg, E. (2017). Trade-off between transcriptome plasticity and genome evolution in cephalopods. Cell *169*, 191–202.e11. https://doi.org/10.1016/j.cell.2017.03.025.

21. Rosenthal, J.J.C., and Bezanilla, F. (2002). Extensive editing of mRNAs for the squid delayed rectifier K+ channel regulates subunit tetramerization. Neuron *34*, 743–757. https://doi.org/10.1016/S0896-6273(02)00701-8.

22. Vallecillo-Viejo, I.C., Liscovitch-Brauer, N., Diaz Quiroz, J.F., Montiel-Gonzalez, M.F., Nemes, S.E., Rangan, K.J., Levinson, S.R., Eisenberg, E., and Rosenthal, J.J.C. (2020). Spatially regulated editing of genetic information within a neuron. Nucleic Acids Res. *48*, 3999–4012. https://doi.org/10.1093/nar/gkaa172.

23. Albertin, C.B., Medina-Ruiz, S., Mitros, T., Schmidbaur, H., Sanchez, G., Wang, Z.Y., Grimwood, J., Rosenthal, J.J.C., Ragsdale, C.W., Simakov, O., et al. (2022). Genome and transcriptome mechanisms driving cephalopod evolution. Nat. Commun. *13*, 2427. https://doi.org/10.1038/s41467-022-29748-w.

24. Crawford, K., Diaz Quiroz, J.F., Koenig, K.M., Ahuja, N., Albertin, C.B., and Rosenthal, J.J.C. (2020). Highly efficient knockout of a squid pigmentation gene. Curr. Biol. *30*, 3484–3490.e4. https://doi.org/10.1016/j.cub.2020.06.099.

25. Jereb, P., and Roper, C. (2005). Cephalopods of the World, Fourth Edition (Food and Agriculture Organization).

26. Jolly, J., Hasegawa, Y., Sugimoto, C., Zhang, L., Kawaura, R., Sanchez, G., Gavriouchkina, D., Marlétaz, F., and Rokhsar, D. (2022). Lifecycle, culture, and maintenance of the emerging cephalopod models *Euprymna berryi* and *Euprymna morsei*. Front. Mar. Sci. *9*, https://doi.org/10.3389/fmars.2022.1039775.

27. Gavriouchkina, D., Tan, Y., Ziadi-Künzli, F., Hasegawa, Y., Piovani, L., Zhang, L., Sugimoto, C., Luscombe, N., Marlétaz, F., and Rokhsar, D.S. (2022). A single-cell atlas of bobtail squid visual and nervous system highlights molecular principles of convergent evolution. Preprint at bioRxiv. https://doi.org/10.1101/2022.05.26.490366.

28. Choe, S. (1966). On the eggs, rearing, habits of the fry, and growth of some Cephalopoda. Bull. Mar. Sci. *16*, 330–348.

29. Sanchez, G., Jolly, J., Reid, A., Sugimoto, C., Azama, C., Marlétaz, F., Simakov, O., and Rokhsar, D.S. (2019). New bobtail squid (Sepiolidae: Sepiolinae) from the Ryukyu islands revealed by molecular and morphological analysis. Commun. Biol. *2*, 465. https://doi.org/10.1038/s42003-019-0661-6.

30. Sanchez, G., Fernández-Álvarez, F.Á., Taite, M., Sugimoto, C., Jolly, J., Simakov, O., Marlétaz, F., Allcock, L., and Rokhsar, D.S. (2021). Phylogenomics illuminates the evolution of bobtail and bottletail squid (order Sepiolida). Commun. Biol. *4*, 819. https://doi.org/10.1038/s42003-021-02348-y.

31. Cloney, R.A., and Brocco, S.L. (1983). Chromatophore organs, reflector cells, iridocytes and leucophores in cephalopods. Am. Zool. *23*, 581–592. https://doi.org/10.1093/icb/23.3.581.

32. van den Branden, C., and Decleir, W. (1976). A study of the chromatophore pigments in the skin of the cephalopod Sepia officinalis. Biol. Jaarb. 345–352.

33. Figon, F., and Casas, J. (2019). Ommochromes in invertebrates: biochemistry and cell biology. Biol. Rev. Camb. Philos. Soc. *94*, 156–183. https://doi.org/10.1111/brv.12441.

34. Aubourg, S.P., Torres-Arreola, W., Trigo, M., and Ezquerra-Brauer, J.M. (2016). Partial characterization of jumbo squid skin pigment extract and its antioxidant potential in a marine oil system. Eur. J. Lipid Sci. Technol. *118*, 1293–1304. https://doi.org/10.1002/ejlt.201500356.

35. Schwinck, I. (1953). Über den Nachweis eines Redox-Pigmentes (Ommochrom) in der Haut von Sepia officinalis. Naturwissenschaften *40*, 365. https://doi.org/10.1007/BF00589572.

36. Williams, T.L., DiBona, C.W., Dinneen, S.R., Labadie, S.F., Chu, F., and Deravi, L.F. (2016). Contributions of phenoxazone-based pigments to the structure and function of nanostructured granules in squid chromatophores. Langmuir *32*, 3754–3759. https://doi.org/10.1021/acs.langmuir.6b00243.

37. Lee, P.N., Callaerts, P., and de Couet, H.G. (2009). Culture of Hawaiian bobtail squid (*Euprymna scolopes*) embryos and observation of normal development. Cold Spring Harb. Protoc. *2009*. pdb.prot5323. https://doi.org/10.1101/pdb.prot5323.

38. Takikawa, O., Yoshida, R., Kido, R., and Hayaishi, O. (1986). Tryptophan degradation in mice initiated by indoleamine 2,3-dioxygenase. J. Biol. Chem. *261*, 3648–3653. https://doi.org/10.1016/S0021-9258(17)35696-X.

39. Suzuki, T. (1994). Abalone myoglobins evolved from indoleamine dioxygenase: the cDNA-derived amino acid sequence of myoglobin from Nordotis madaka. J. Protein Chem. *13*, 9–13.

40. Suzuki, T., Yokouchi, K., Kawamichi, H., Yamamoto, Y., Uda, K., and Yuasa, H.J. (2003). Comparison of the sequences of Turbo and Sulculus indoleamine dioxygenase-like myoglobin genes. Gene *308*, 89–94. https://doi.org/10.1016/S0378-1119(03)00467-0.

41. Yuasa, H.J., and Suzuki, T. (2005). Do molluscs possess indoleamine 2,3-dioxygenase? Comp. Biochem. Physiol. B Biochem. Mol. Biol. *140*, 445–454. https://doi.org/10.1016/j.cbpc.2004.11.007.

42. Suzuki, T., Kawamichi, H., and Imai, K. (1998). A myoglobin evolved from indoleamine 2,3-dioxygenase, a tryptophan-degrading enzyme. Comp. Biochem. Physiol. B Biochem. Mol. Biol. *121*, 117–128. https://doi.org/10.1016/S0305-0491(98)10086-X.

43. Kawamichi, H., and Suzuki, T. (1998). The cDNA-derived amino acid sequence of indoleamine dioxygenase like-myoglobin from the gastropod mollusc Omphalius pfeifferi. J. Protein Chem. *17*, 651–656. https://doi.org/10.1007/BF02780966.

44. Pungor, J.R., Allen, V.A., Songco-Casey, J.O., and Niell, C.M. (2023). Functional organization of visual responses in the octopus optic lobe. Preprint at bioRxiv. https://doi.org/10.1101/2023.02.16.528734.

45. Margaret J, M. (1999). Consequences of evolving with bacterial symbionts: insights from the squid-vibrio associations. Annu. Rev. Ecol. Syst. *30*, 235–256. https://doi.org/10.1146/annurev.ecolsys.30.1.235.

46. Belcaid, M., Casaburi, G., McAnulty, S.J., Schmidbaur, H., Suria, A.M., Moriano-Gutierrez, S., Pankey, M.S., Oakley, T.H., Kremer, N., Koch, E.J., et al. (2019). Symbiotic organs shaped by distinct modes of genome evolution in cephalopods. Proc. Natl. Acad. Sci. USA *116*, 3030–3035. https://doi.org/10.1073/pnas.1817322116.

47. Cristina, B., Veronica, R., Silvia, A., Andrea, G., Sara, C., Luca, P., Nicoletta, B., M C, B.J., Silvio, B., and Fabio, T. (2022). Identification and characterization of the kynurenine pathway in the pond snail Lymnaea stagnalis. Sci. Rep. *12*, 15617. https://doi.org/10.1038/s41598-022-19652-0.

48. Chen, L.M., Bao, C.H., Wu, Y., Liang, S.H., Wang, D., Wu, L.Y., Huang, Y., Liu, H.R., and Wu, H.G. (2021). Tryptophan-kynurenine metabolism: a link between the gut and brain for depression in inflammatory bowel disease. J. Neuroinflammation *18*, 135. https://doi.org/10.1186/s12974-021-02175-2.

49. Huang, Y.S., Ogbechi, J., Clanchy, F.I., Williams, R.O., and Stone, T.W. (2020). IDO and kynurenine metabolites in peripheral and CNS disorders. Front. Immunol. *11*, 388. https://doi.org/10.3389/fimmu.2020.00388.

50. Modoux, M., Rolhion, N., Mani, S., and Sokol, H. (2021). Tryptophan metabolism as a pharmacological target. Trends Pharmacol. Sci. *42*, 60–73. https://doi.org/10.1016/j.tips.2020.11.006.

51. Wang, Q., Liu, D., Song, P., and Zou, M.H. (2015). Tryptophan-kynurenine pathway is dysregulated in inflammation and immune activation. Front. Biosci. (Landmark Ed) *20*, 1116–1143.

52. Prendergast, G.C., Malachowski, W.J., Mondal, A., Scherle, P., and Muller, A.J. (2018). Indoleamine 2,3-dioxygenase and its therapeutic inhibition in cancer. Int. Rev. Cell Mol. Biol. *336*, 175–203. https://doi.org/10.1016/bs.ircmb.2017.07.004.

53. Too, L.K., Li, K.M., Suarna, C., Maghzal, G.J., Stocker, R., McGregor, I.S., and Hunt, N.H. (2016). Deletion of TDO2, IDO-1 and IDO-2 differentially affects mouse behavior and cognitive function. Behav. Brain Res. *312*, 102–117. https://doi.org/10.1016/j.bbr.2016.06.018.

54. Styfhals, R., Zolotarov, G., Hulselmans, G., Spanier, K.I., Poovathingal, S., Elagoz, A.M., de Winter, S., Deryckere, A., Rajewsky, N., Ponte, G., et al. (2022). Cell type diversity in a developing octopus brain. Nat. Commun. *13*, 7392. https://doi.org/10.1038/s41467-022-35198-1.

55. Songco-Casey, J.O., Coffing, G.C., Piscopo, D.M., Pungor, J.R., Kern, A.D., Miller, A.C., and Niell, C.M. (2022). Cell types and molecular architecture of the Octopus bimaculoides visual system. Curr. Biol. *32*, 5031–5044.e4. https://doi.org/10.1016/j.cub.2022.10.015.

56. Qian, Y., Li, J., Zhao, S., Matthews, E.A., Adoff, M., Zhong, W., An, X., Yeo, M., Park, C., Yang, X., et al. (2022). Programmable RNA sensing for cell monitoring and manipulation. Nature *610*, 713–721. https://doi.org/10.1038/s41586-022-05280-1.

57. Dereeper, A., Guignon, V., Blanc, G., Audic, S., Buffet, S., Chevenet, F., Dufayard, J.F., Guindon, S., Lefort, V., Lescot, M., et al. (2008). Phylogeny.fr: robust phylogenetic analysis for the non-specialist. Nucleic Acids Res. *36*, W465–W469. https://doi.org/10.1093/nar/gkn180.

58. Rambaut, A. (2018). FigTree. http://tree.bio.ed.ac.uk/software/figtree/.

59. Price, M.N., Dehal, P.S., and Arkin, A.P. (2010). FastTree 2 – approximately maximum-likelihood trees for large alignments. PLoS One *5*, e9490. https://doi.org/10.1371/journal.pone.0009490.

60. The MathWorks Inc. (2021). Scanbox software package for MATLAB.

61. Brainard, D.H. (1997). The psychophysics toolbox. Spat. Vis. *10*, 433–436. https://doi.org/10.1163/156856897X00357.

62. Abbo, L.A., Himebaugh, N.E., DeMelo, L.M., Hanlon, R.T., and Crook, R.J. (2021). Anesthetic efficacy of magnesium chloride and ethyl alcohol in temperate octopus and cuttlefish species. J. Am. Assoc. Lab. Anim. Sci. *60*, 556–567. https://doi.org/10.30802/AALAS-JAALAS-20-000076.

63. Grearson, A.G., Dugan, A., Sakmar, T., Sivitilli, D.M., Gire, D.H., Caldwell, R.L., Niell, C.M., Dölen, G., Wang, Z.Y., and Grasse, B. (2021). The lesser pacific striped octopus, *Octopus chierchiae*: an emerging laboratory model. Front. Mar. Sci. *8*, 753483. https://doi.org/10.3389/fmars.2021.753483.

64. Shomrat, T., Zarrella, I., Fiorito, G., and Hochner, B. (2008). The octopus vertical lobe modulates short-term learning rate and uses LTP to acquire long-term memory. Curr. Biol. *18*, 337–342. https://doi.org/10.1016/j.cub.2008.01.056.

65. Niell, C.M., and Smith, S.J. (2005). Functional imaging reveals rapid development of visual response properties in the zebrafish tectum. Neuron *45*, 941–951. https://doi.org/10.1016/j.neuron.2005.01.047.

66. Koizumi, M., Shigeno, S., Mizunami, M., and Tanaka, N.K. (2018). Calcium imaging method to visualize the spatial patterns of neural responses in the pygmy squid, Idiosepius paradoxus, central nervous system. J. Neurosci. Methods *294*, 67–71. https://doi.org/10.1016/j.jneumeth.2017.11.009.

Please cite this article in press as: Ahuja et al., Creation of an albino squid line by CRISPR-Cas9 and its application for *in vivo* functional imaging of neural activity, Current Biology (2023), https://doi.org/10.1016/j.cub.2023.05.066

STAR★METHODS

KEY RESOURCES TABLE

REAGENT or RESOURCE	SOURCE	IDENTIFIER
Chemicals, peptides, and recombinant proteins		
Penicillin-Streptomycin 100x	GIBCO	15-140-122
2X NLS Cas9 protein	Synthego	N/A
Agarose, Type II-A, Medium EEO	Sigma-Aldrich	A9918
Paraformaldehyde	Electron microscopy sciences	15714
Diethyl pyrocarbonate	Sigma-Aldrich	D5758
Fluoromount-G	Southern biotech	0100-20
Trizol	Invitrogen	15596026
Probe wash buffer	Molecular Instruments	N/A
Probe hybridization buffer	Molecular Instruments	N/A
Hairpins	Molecular Instruments	B1-647
Critical commercial assays		
Monarch DNA Kit	NEB	T3010L
Monarch Gel Extraction kit	NEB	T2010L
Invitrogen Qubit dsDNA HS Assay kit	Invitrogen	Q32850
cDNA SuperScript kit	Invitrogen	11904018
Experimental models: Organisms/strains		
Euprymna berryi TDO KO	MBL	N/A
Euprymna berryi IDO KO	MBL	N/A
Euprymna berryi TDO/IDO KO	MBL	N/A
Euprymna berryi WT broodstock	MBL	N/A
Oligonucleotides		
TDO qpcr fwd	IDT	TTATCGAGATGAGCCGAGGT
TDO qpcr rev	IDT	CACTTTGTAACGGTCGCTGA
IDO qpcr fwd	IDT	AAACGAAGGAGTTTCGAGCA
IDO qpcr rev	IDT	GCCAGACACTTGGGAATCAT
EB TDO F3	IDT	CTTAGAGCTGGTTAGAACGCACC
EB TDO R3	IDT	GGCAAACAAATCTTACCTGAGCAGG
EB IDO F3	IDT	CCTTTTGGTTATTCAGATGTCTCAGC
EB IDO R3	IDT	GTTAACTTACGTGTGGAACACCG
Probes for TDO	Molecular Instruments	N/A
Probes for IDO	Molecular Instruments	N/A
CRISPR sgRNAs		
TDO gRNA 1	Synthego	GGAAGCUGUUGAUUGUUGGU
TDO gRNA 2	Synthego	GGCUGGUUAGAACGCACCCC
TDO gRNA 3	Synthego	GGAGAAUGAUCCAAAGAAAA
IDO gRNA 1	Synthego	GGUGAGCCAGGUGCUUCUCG
IDO gRNA 2	Synthego	GGAGGUUAUGUGUGGCAAAA
Software and algorithms		
MUSCLE	Dereeper et al.[57]	RRID: SCR_011812
Fig tree Software	Rambaut[58]	http://tree.bio.ed.ac.uk/software/figtree
Fast tree 2 software	Price et al.[59]	http://www.microbesonline.org/fasttree/
BLAST	NCBI	RRID: SCR_004870
Scanbox software package for MATLAB	Mathworks[60]	N/A
PsychToolbox package for MATLAB	Brainard[61]	RRID: SCR_002881

(*Continued on next page*)

Please cite this article in press as: Ahuja et al., Creation of an albino squid line by CRISPR-Cas9 and its application for *in vivo* functional imaging of neural activity, Current Biology (2023), https://doi.org/10.1016/j.cub.2023.05.066

Continued

REAGENT or RESOURCE	SOURCE	IDENTIFIER
Indel.py	Crawford et al.[24]	https://github.com/pipedq/CRISPR_G0_Genotyping
Cumulative.py	Crawford et al.[24]	https://github.com/pipedq/CRISPR_G0_Genotyping
Event_frequency.py	Crawford et al.[24]	https://github.com/pipedq/CRISPR_G0_Genotyping
Other		
Quartz glass capillaries for making injection needles	Sutter Instruments	QF100-70-10
Egg laying structure	Imagitarium Resin Rustic Tower Aquatic Décor, Petco, USA	N/A
recording chamber consisted of a plastic box with one side replaced with white diffusing glass	TAP Plastics & Edmund Optics	02-149- white diffusing glass
1" pieces of 16 gauge insulated wire	N/A	N/A

RESOURCE AVAILABILITY

Lead contact

Further information and requests for resources and reagents should be directed to and will be fulfilled by the lead contact, Dr. Joshua Rosenthal (jrosenthal@mbl.edu).

Materials availability

This study did not generate new reagents.

Data and code availability

The scripts (Cumulative.py, indels.py, Event_frequency.py) used in this study are listed in the key resources table are the same as in Crawford et al.[24] and are available at Github (https://github.com/pipedq/CRISPR_G0_Genotyping). Reads from the amplicon sequencing will be shared by the lead contact on request. Any additional information required to reanalyze the data reported in this paper is available from the lead contact upon request.

EXPERIMENTAL MODEL AND SUBJECT DETAILS

Euprymna berryi were cultured through their life cycle at the Marine Resources Center at the Marine Biological Laboratory, Woods Hole, MA. Wild type male and female squid were kept in breeding tanks. For the CRISPR knockout lines, males and females with deletions were kept in separate tanks until ready for crossing when they were put in a tank together to breed. Details on the culturing and information relating to genotype, sex and developmental stage can either be found below or by contacting the lead contact Dr. Joshua Rosenthal (jrosenthal@mbl.edu).

Imaging experiments were performed at University of Oregon, with oversight provided by the Institutional Animal Care and Use Committee. After being delivered to University of Oregon, animals were kept in a closed circulating 250-gallon aquarium system in artificial seawater and used for experiments by one week after hatching.

All husbandry and experimental protocols were in accordance with the EU 2010/63/EU[99] and AAALAC guidelines for the use and care of cephalopods for research.

METHOD DETAILS

Embryo collection and preparation

In our breeding system, mated females lay their eggs during the night by attaching them under rocks, on shells or artificial structures, or in the corners of the tank. Eggs were harvested in the early morning and removed from their substrate by gently scraping them with dull, large forceps into a bucket of filtered seawater. Upon extrusion from the female, each *E. berryi* embryo is wrapped in 2 different types of jelly, each with a different consistency. The outer, yellow-brown jelly is relatively hard and forms a single layer. Below this, the inner jelly forms 20-30 fine layers and is soft and very sticky. Both jelly layers are removed from the eggs for injection under a dissecting microscope using Number 5 Dumont forceps. Embryos are fragile so care must be exercised when removing the inner jelly layers in order not to damage the early cells or yolk. Only portions of the egg clutches were used for microinjections. The remainders were held in 4-liter tanks in the mariculture systems as sibling controls.

Please cite this article in press as: Ahuja et al., Creation of an albino squid line by CRISPR-Cas9 and its application for *in vivo* functional imaging of neural activity, Current Biology (2023), https://doi.org/10.1016/j.cub.2023.05.066

Embryo Injection

For microinjection, embryos were stabilized in troughs made in agarose dishes. To make the troughs, 10 cm plastic petri dishes were filled with molten 1% type II agarose in which two 1'' pieces of 16 gauge insulated wire is placed. Once hardened, the wire was gently removed, and the resulting two troughs approximated the diameter of the embryos. Dishes were then filled with sterile filtered seawater, and de-jellied embryos were gently pushed into the troughs with fine forceps with the blastomere facing up. Injection needles were made using 1 mm O.D./ 0.7 mm I.D. quartz capillaries (Sutter Instruments, Novato, CA QF100-70-10) and a P-2000 laser puller (Sutter Instruments, Novato, CA) with the following single-step program: heat 750, filament 4, velocity 60, delay 140 and pull 200. Injection needles were then beveled at a 20° angle with one full clockwise rotation for 30 seconds on a BV-10 beveler (Sutter Instruments, Novato, CA), to produce a tip diameter of 3-4 mm. Needles were backfilled with 1-2 μl of injection mix and each embryo was injected with 0.22 pL using a Xenoworks Digital Pressure Injector (Sutter Instruments, Novato CA), an MN-153 micro manipulator (Narishige USA) and a V8 Discovery stereoscope (Zeiss Instruments).

CRISPR-Cas9 injection mixes

For TDO and TDO+IDO injections, the injection mix consisted of 33 μM total CRISPR gRNA (11 μM of each using 3 gRNAs), 7 μM Cas9 protein (2x NLS Cas9, Synthego Corporation) and 1.7X PBS. We estimate that 3.76 amol of each sgRNA and 1.54 amol of Cas9 protein were injected per embryo. For IDO injections, embryos were injected with 33 μM total gRNA (16.5 μM each since only 2 were used), 7 μM Cas9 protein and 1.7X PBS. We estimate that 5.64 amol of each sgRNA was injected. Chemically protected CRISPR gRNAs, synthesized by Synthego Corporation (Redwood City, CA), had the following sequences: TDO gRNA 1 GGAAGCUG UUGAUUGUUGGU, TDO gRNA 2 GGCUGGUUAGAACGCACCCC, TDO gRNA 3 GGAGAAUGAUCCAAAGAAAA, IDO gRNA 1 GGU GAGCCAGGUGCUUCUCG, IDO gRNA 2 GGAGGUUAUGUGUGGCAAAA. CRISPR gRNAs were modified by the manufacturer with 2'-O-methyl groups on the first and last three bases and 3' phosphorothioate linkages between the first three and last two bases. These modifications are reported to protect the gRNAs from exonucleases, and thereby improve efficiency and reduce off-target cuts.

Identifying TDO and IDO in *E. berryi*

The human TDO and IDO protein sequences were used as bait to search the proteomes of *E. berryi*, *E. scolopes*, *D. pealeii, Octopus bimaculoides, Architeuthis dux, Crassostrea gigas, Capitella teleta*, *Drosophila melanogaster*, *Tribolium castaneum*, and *Mus musculus* using BLAST [NCBI]. Candidate IDO and TDO sequences were aligned using MUSCLE[57] and an approximately maximum likelihood tree was built with FastTree2[59] and illustrated with FigTree[58] (see also Figure S1).

Hybridization Chain Reaction

Probes for IDO and TDO were ordered from Molecular Instruments (Los Angeles, CA) based on the predicted cDNA sequence from the *E. berryi* genome. Embryos were anesthetized in a 1:1 dilution of 7.5% MgCl2 in filtered natural seawater[62] and fixed overnight at 4°C in 4% paraformaldehyde (Electron Microscopy Science 15714) in filtered seawater. Fixed embryos were washed twice for 5 minutes and then twice for 30 minutes in diethyl pyrocarbonate (DEPC)-treated PBS with 1% tween20 (Sigma, St. Louis MO) and stored in a hybridization solution (50% formamide, 5xSSC, 1% SDS, 250g yeast tRNA, and 0.1g heparin sulfate per 500mL) at -20°C until use. Tissue was warmed to room temperature and moved into probe hybridization buffer (PHB; Molecular Instruments). Embryos were then prehybridized in 150 μL of PHB for 1h at 37 degrees C. The prehybridization buffer was removed and replaced with 150 μl PHB with 3 pmol of each probe and incubated overnight at 37°C. Excess probe was removed by washing twice for 5 minutes, four times for 30 minutes, and once for one hour with wash buffer (Molecular Instruments) at 37°C. Embryos were then washed twice for 5 minutes with 5xSSCT (5x SSC with 1% Tween) and pre-amplified with 150 μL amplification buffer for 30 minutes at room temperature. Separately, 9pmol each of hairpin H1 and H2 (Molecular Instruments) were heated to 95°C for 90 seconds and cooled to room temperature in the dark for 30 minutes. Hairpin solutions were diluted in 150 μL of amplification buffer and used to replace the preamplification buffer. Embryos were incubated overnight in the dark at room temperature. Excess hairpins were removed by washing twice for 5 minutes, and three times for 30 minutes in 5xSSCT and were stored in the dark at 4°C until imaging. Samples were imaged in Fluoromount-G with DAPI (Southern Biotech) on a LSM 710 confocal (Zeiss).

Quantification of TDO and IDO expression by qPCR

Stage 24 *E. berryi* embryos were anesthetized as described above and flash frozen in liquid nitrogen prior to RNA isolation using Trizol (Invitrogen 15596026) following the manufacturer's protocol. RNA integrity was verified on an agarose gel. First strand cDNA synthesis was generated with the SuperScript kit (Invitrogen 11904018) following manufacturer's protocols. All primer pairs were tested for amplification efficiency by making three ten-fold serial dilutions of cDNA from one stage 24 *E. berryi* embryo. Reactions were performed in triplicate using NEB Luna Universal qPCR Master Mix (M300L) and run on Applied Biosystems StepOnePlus Real-Time PCR System. Both primer pairs had an efficiency > 0.95. The primer sequences for TDO were TTATCGAGATGAGCCGAGGT and CACTTTGTAACGGTCGCTGA and for IDO were AAACGAAGGAGTTTCGAGCA and GCCAGACACTTGGGAATCAT. To determine the relative expression of TDO and IDO (Figure 3B), qPCR amplifications were performed on cDNA from 5 different animals at two dilutions. The relative expression presented in the text was calculated as follows: Exp(TDO)/Exp(IDO) = $2^{Cp(TDO)-Cp(IDO)}$.

Please cite this article in press as: Ahuja et al., Creation of an albino squid line by CRISPR-Cas9 and its application for *in vivo* functional imaging of neural activity, Current Biology (2023), https://doi.org/10.1016/j.cub.2023.05.066

Genotyping

For F1 animals and beyond, genotyping was performed by PCR using primers that spanned the TDO or IDO CRISPR-directed Cas9 cut sites. For hatchlings, genomic DNA was extracted from whole animals using the NEB Monarch gDNA purification kit (CAT #T3010L). For juveniles destined for breeding genetic lines, 1-2 month old animals were gently swabbed with a Puritan sterile foam tipped applicator using 10 strokes on their dorsal and ventral sides of the mantle. DNA was extracted from the swab using the same kit and used to perform PCR amplifications for regions spanning the gRNA target sites. The primer pair EB TDO F3 (CTTAGAGCTGGTTAGAACGCACC) and EB TDO R3 (GGCAAACAAATCTTACCTGAGCAGG) were used resulting in a 132bp amplicon. The primer pair EB IDO F3 (CCTTTTGGTTATTCAGATGTCTCAGC) and EB IDO R3 (GTTAACTTACGTGTGGAACACCG) were used resulting in a 146bp amplicon. PCR products were run on 2% agarose gels and bands were purified using the NEB gel extraction kit (CAT #T1020L). These were quantified using Invitrogen Qubit dsDNA HS Assay kit (CAT #Q32850) and sent for Sanger Sequencing using the service provided by Genewiz (South Plainfield, NJ). To estimate TDO disruption in G0 animals, PCR amplicons spanning the TDO target sites were sequenced on the MiSeq platform using the Amplicon EZ service at Genewiz (South Plainfield, NJ). Details of MiSeq analyses and the scripts used are identical to those reported previously in 2020.[24]

E. berryi embryo culture

Embryos were cultured in 60 mm plastic petri dishes with sterile filtered sea water and Pen-Strep at a 1:100 dilution (Gibco, USA). This incubation media was oxygenated by vigorous shaking before being added to the dishes. Embryos were cultured at $\leq$25/dish at 24°C. Seawater was changed every other day and dead embryos were promptly removed. Juvenile and adult animals were cultured in the seawater system described in Grearson et al.[63] Sexually mature animals were held in fiberglass A-frame system ranging from 80 to 100 gallons. The female to male ratio was kept at 3:1. A layer of 0.25" – 0.5" deep coarse sand covered the entire bottom of the tank to allow the animals to bury themselves. Each tank had one egg laying structure (Imagitarium Resin Rustic Tower Aquatic Décor, Petco, USA) per female. These structures were 3 -4" off the sand with only one entrance/exit. A heavy rock was placed on top of the egg laying structure to provide a stable environment. Females laid approximately one clutch of eggs per week.

Some eggs were removed from the system and used for microinjections; others, however, were used to maintain genetic lines. These were kept in the mariculture systems in a 4-liter tank. The eggs were placed in a 4" square aquaponic 1.5 mm mesh plant basket. The basket was attached to the side of the tank using a suction cup ½" – 1" below the water surface and ½" – 1" away from the tank sea water supply line. This placement allows for ideal passive flow across the whole clutch. Maintenance and removal of nonviable eggs were performed daily. To prevent any eggs or hatchlings from escaping the tank, a 1mm fine mesh screen was placed over the tank discharge. Once eggs hatch, a thin layer of fine sand is added to the bottom of the tank and the tank sides are blacked out to reduce visual stimuli and stress. Hatchlings were then transferred to independent enclosures with a wide-mouth glass dropper. Individuals were raised in 4" opaque 2qt round polyethylene containers with positive-lock lids to ensure isolated genetics were maintained. Water flow and aeration of these enclosures were carefully administered to maintain ideal conditions. Each enclosure received precise flow-through seawater supply utilizing 0.5 gal/hr (1.9L/hr) drip irrigation emitters. Water exited through custom ½" ports with 1000-micron mesh screening near the top of each enclosure. Consistent aeration for each enclosure was controlled from an ¼" barb shut-off valve to give a flow rate of 1 bubble every 3 seconds. Within the first 12 hours, hatchlings were phototactic but did not exhibit feeding behavior until 24-hour post hatching. All hatchlings were fed a strict diet of enriched *Americamysis bahia* and the quantity of food was adjusted as the hatchlings grew. Once hatchlings were a month old, they were transitioned onto *Palaemonetes pugio* and the tank enclosure was increased. Feeding schedule was increased in conjunction with the increased feeding response, up to and through sexual maturity.

Calcium Dye Injection

Animals were deeply anesthetized in artificial sea water (ASW) (460mM NaCl2, 10mM KCl, 10mM glucose, 10mM HEPES, 55mM MgCl2, 11mM CaCl2, 2mM glutamine), additionally supplemented to contain 110mM MgCl2 to induce anesthesia[64] for the duration of the injection. Animals were attached to a coverslip using Vetbond adhesive (3M), and further secured under a thin layer of 4% low melt agarose (Sigma) to minimize movement. A small incision was opened through the skin to allow for the penetration of a quartz beveled needle, prepared as described above, into the optic lobe. Needles were backfilled with a dye solution of 1mM Cal-520 AM (AAT Bioquest), 2.5% Alexa Fluor 568 Hydrazide (Thermo Fisher), 8% dimethylsulfoxide, and 2% pluronic acid (AAT Bioquest) in ASW. Dye was pressure injected into one optic lobe with an MPPI-3 Pressure Injector from Applied Science Instrumentation. This paradigm was adapted from previous work in zebrafish.[65,66]

After injection, the preparation was moved to a recording chamber filled with ASW. The recording chamber consisted of a plastic box (TAP Plastics) with one side replaced with white diffusing glass (Edmund Optics Cat. Num. 02-149) to serve as a projection screen for visual stimuli. The preparation was placed on a custom-built rotatable platform within the recording chamber to allow for alignment of the preparation to the stimulus screen. The chamber temperature was monitored and held between 17 and 19°C, and continually oxygenated via an airstone.

Calcium imaging was performed using a two-photon microscope (Neurolabware). Data were acquired using the Scanbox software package for MATLAB.[60] Responses were identified using custom software in MATLAB, to extract fluorescence traces from defined ROIs and align this with stimulus timing.

Please cite this article in press as: Ahuja et al., Creation of an albino squid line by CRISPR-Cas9 and its application for *in vivo* functional imaging of neural activity, Current Biology (2023), https://doi.org/10.1016/j.cub.2023.05.066

Visual stimuli

Visual stimuli were presented using the PsychToolbox[61] package for MATLAB and displayed with a pico LCD projector (AAXA Technologies) onto the diffusion filter on the side of the recording chamber. A stimulus of square gratings at 0.01 and 0.16 cyc/deg spatial frequency, 2 Hz temporal frequency, in one of eight directions motion (0-315 degrees at 45-degree intervals) were presented for one second, with an inter-stimulus interval of two seconds of a gray (50% luminance) screen.

QUANTIFICATION AND STATISTICAL ANALYSIS

We used amplicon sequencing and our own code to analyze the percent disruption of TDO in TDO knockout G0 *Euprymna berryi* squid. The details of this sequencing can be found in the method details below. The code used to perform the analysis is the same as that in previous work,[24] which is also addressed in the STAR Methods and key resources table. The analysis of TDO disruption in these animals is summarized in Figure 1 and its legend. To quantify the amount of *tdo* and *ido* expression in *Euprymna berryi* we used qPCR. The explicit details of these experiments and analysis can be found in both the Figure 3 legend and the method details section below, including how the experiment was run, the number of replicates and the formula used to calculate relative expression. For the calcium imaging experiments we used online software and customized versions of software to analyze subsequent responses to these experiments, which are detailed below in the methods section, including which software was used and how experiments were performed. Our visual analysis of these experiments and orientation of the animals are shown in Figures 5 and 6 and are explained in the corresponding figure legends.

Current Biology, Volume *33*

Supplemental Information

Creation of an albino squid line by CRISPR-Cas9 and its application for *in vivo* functional imaging of neural activity

Namrata Ahuja, Ernie Hwaun, Judit R. Pungor, Ruhina Rafiq, Sal Nemes, Taylor Sakmar, Miranda A. Vogt, Bret Grasse, Juan Diaz Quiroz, Tessa G. Montague, Ryan W. Null, Danielle N. Dallis, Daria Gavriouchkina, Ferdinand Marletaz, Lisa Abbo, Daniel S. Rokhsar, Cristopher M. Niell, Ivan Soltesz, Caroline B. Albertin, and Joshua J.C. Rosenthal

S1

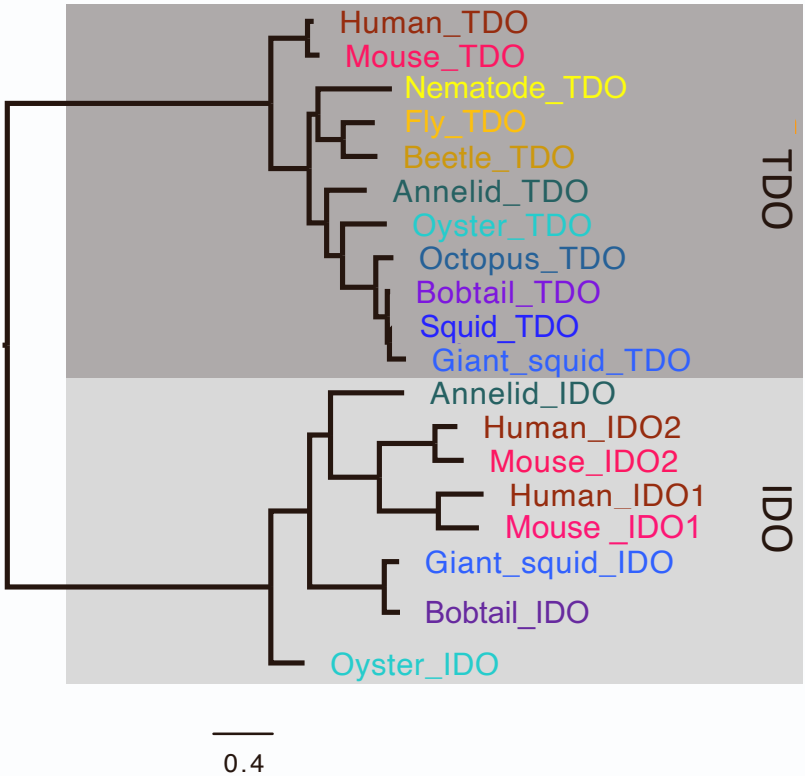

Supplementary Figure 1. Approximate maximum likelihood phylogenetic tree of TDO and IDO protein sequences identified from select species spanning bilaterian groups. Names are colored according to phylum, with vertebrates (human and mouse) in shades of red, arthropods (*Drosophila* and the beetle *Tribolium*) in orange, the nematode *C. elegans* in yellow, the annelid *Capitella spp.* in teal, the oyster *Crassostrea gigas* in sky blue, and the cephalopods *Octopus bimaculoides, Doryteuthis pealeii, Architeuthis dux,* and *Euprymna berryi* in blues and purples. *Euprymna* (purple) genomes encode both TDO and IDO, but we could not identify an IDO sequence in the *D. pealeii* genome. Scale bar indicates changes per site.